



Hard particle spectra from parallel shocks due to turbulence transmission

JONI TAMMI

UCD School of Mathematical Sciences, University College Dublin, Dublin 4, Ireland

joni.tammi@iki.fi

Abstract: If taken into account, the transmission of the particle-scattering turbulence –in addition to just the particles– through the shock front can change the effective compression ratio felt by the accelerating particles significantly from the compression of the underlying plasma. This can lead to significantly harder energy spectra than what are traditionally predicted assuming frozen-in turbulence. I consider the applicability and limitations of turbulence transmission scenario in parallel shock waves of different thickness, its consequences in AGN and microquasar environments, and discuss the possible effects to the spectrum of the accelerated particles.

Introduction

The first-order Fermi acceleration process in shock waves is often considered as the main mechanism responsible for the nonthermal electron populations assumed to produce the observed radiation in many astrophysical sources. In the basic theory particles gain energy scattering elastically off magnetic turbulence –e.g., Alfvén waves– frozen-in to the converging flow. The process is known to accelerate charged particles to power-law energy distributions $N \propto E^{-\sigma}$, with spectral index σ having value ~ 2 for nonrelativistic and ~ 2.2 for relativistic shocks, fitting many observations.

For the simplest nonrelativistic (unmodified) step shocks the spectral index of the accelerated particles is known to depend mainly on the compression ratio of the plasma, $r \simeq r_{\text{flow}} = V_1/V_2$, as $\sigma = \frac{r+2}{r-1}$, where V_1 and V_2 are the shock-frame speeds of the far up- and downstream flows, respectively. The compression ratio itself depends on the hydrodynamics of the flow, and has values ranging from 4 (nonrelativistic) to 3 (for $V_1 \rightarrow c$). In modified thicker shocks the effect of broadened speed profile leads to decreased acceleration efficiency and steeper spectra. [1, 2]

Although many observations are in accordance with σ of 2 or 2.2, some sources seem to require significantly smaller indices beyond the limits of the traditional first-order acceleration the-

ory. Although there are other plausible mechanisms capable of producing $\sigma < 2$, omitting the assumption of frozen-in turbulence might be sufficient even for the first-order process alone to allow for hard spectra. Namely, by including the dynamics of the particle-scattering waves –and the effects the shock has on them– in the analysis, one arrives to a situation where the *effective* compression ratio felt by the scattering centres can be significantly higher than that of the underlying flow, r_{flow} . [3–8] In this paper I review recent studies done so far for parallel shocks, discuss the physical requirements for the scenario, and illustrate the effect method in the case of the microquasar Cygnus X-3.

Wave transmission

In very thin astrophysical plasmas particle–particle collisions are extremely rare and the particles only “see” the magnetic turbulence. If this turbulence is frozen-in to the plasma, then the scattering-centre speed is simply that of the underlying plasma flow. But, as has been known for long [9], if the waves themselves have significant speeds with respect to the flow, then also the scattering-centre speed changes. For turbulence consisting of Alfvén waves propagating in the plasma with Alfvén speed V'_A either parallel (“forward”) or antiparallel (“backward”) to the direction of the flow with respect to the shock, the wave speed in the

shock rest frame is simply the flow speed $V(x)$ in the shock frame plus (or minus) the local Alfvén speed in the plasma frame. When there are both wavemodes present, it becomes useful to define the *normalised cross-helicity* of the waves as

$$H_c = \frac{I^+ - I^-}{I^+ + I^-} \in [-1, +1],$$

where $I^\pm \equiv I^\pm(x, k) \propto k^{-q}$ (for $k > k_0$) are the wave spectra of the forward (+) and the backward (−) waves for a given wavenumber at a given location. The “mean scattering-centre speed” is then

$$V_{sc} = \frac{V + H_c V'_A}{1 + H_c V V'_A}.$$

Furthermore, we introduce the the Lorentz factor $\Gamma = 1/\sqrt{1 - V^2/c^2}$ and the *quasi-Newtonian Alfvénic Mach number*,

$$M \equiv \frac{V_1 \Gamma_1}{V'_{A1} \Gamma_{A1}},$$

where the proper Alfvén speed

$$V'_{A1} \Gamma_{A1} = \frac{B}{\sqrt{4\pi\mu n}},$$

and the specific enthalpy $\mu = (\rho + P)/n$ depend on the total energy density ρ , number density n , and the pressure, P , of the gas.

In a super-Alfvénic shock the speed of the flow with respect to the shock is always larger than the local wave speed. In other words, as seen in the shock rest frame, both the forward and backward moving waves propagate toward the shock in the upstream and away from it in the downstream; there are no waves crossing the shock from downstream to upstream. This allows us to define the *critical Mach number* $M_c \equiv \sqrt{r}$, above which the aforementioned conditions are fulfilled. [4]

In order to calculate the scattering-centre speeds on both sides of the shock one has to solve how the shock crossing affects the wavelenghts and amplitudes of the waves. So far this has been done separately for the step shock approximation (i.e., for waves much longer than the shock structure) [3–5] and for thick modified shocks (or for waves sufficiently short, seeing the transition of flow parameters as smooth). [6, 7]

Wave field behind the shock

Details of the transmission process depend on the wavelength of the crossing wave; if the waves are long compared to the shock transition, the part of the waves are simply transmitted through the shock while part is reflected (i.e., “+” waves become “−” waves and vice versa) and regardless of the upstream wave composition there will be both wave modes present in the behind the shock. [3, 4] Different waves are also amplified differently leading to situation where, regardless of the upstream wave field, the waves immediately behind a step shock are flowing predominantly antiparallel to the flow and “following” the shock.

If the shock transition is wide enough to allow for the waves to see it as a smooth change from upstream to downstream plasma parameters, there will in general be no wave reflection case (see, however, e.g. [10]), and an all-forward upstream will result into all-forward downstream and likewise for the backward waves (i.e., $H_{c1} = \pm 1 \Rightarrow H_{c2} \pm 1$). [6, 7] This leads to a qualitative difference compared to the step-shock case as now, depending on the upstream wave field and the shock speed, there are also cases where the downstream cross-helicity (or the “average wave direction”) is positive, i.e., most of the waves are propagating forward (see Fig. 1 in [7]).

Increased compression ratio

From the wave and flow speeds and the cross-helicity on both sides of the shock one can calculate the compression ratio of the scattering centres, $r_k \equiv V_{k1}/V_{k2}$. This is the compression felt by the particles crossing the shock, and it can differ significantly from the compression ratio of the flow r . For $M \rightarrow \infty$ the effective wave speed $V_k \rightarrow V$ and we have usual the frozen-in turbulence, but as $M \rightarrow M_c$ (or, as V'_A becomes non-negligible with respect to V), the scattering-centre compression ratio starts to differ from that of the flow.

Figures 1 and 2 show r_k/r as a function of the Alfvénic Mach number (normalised to the critical value M_c) for different shock speeds; Fig. 1 corresponds to the case with Kolmogorov-type turbulence pre-existing in the upstream ($H_{c1} = 0, q = 5/3$), and Fig. 2 has all waves initially antiparal-

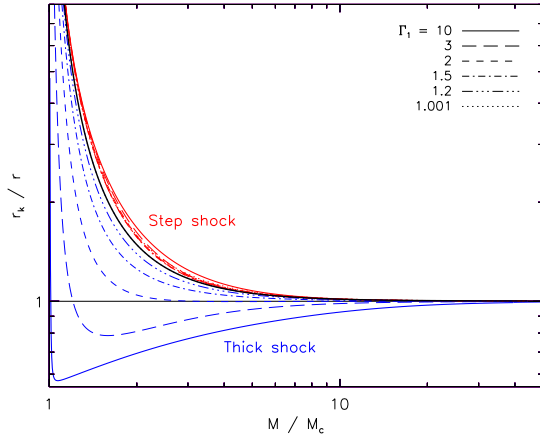


Figure 1: Scattering-centre compression ratio r_k as a function of Alfvénic Mach number M for various shock speeds in the case of upstream turbulence corresponding to $H_{c1} = 0$ and $q = 5/3$. The thick black line separates the step and thick shock cases.

lel to the flow, as if self-generated by high-energy cosmic rays streaming ahead of the shock ($H_{c1} = -1, q = 2$). In Fig. 1 one can also see the case for thick relativistic shocks (or very short waves), where the effective compression ratio can also be decreased. In most cases the compression ratio is, however, increased for magnetic field strengths sufficient to allow for non-negligible wave speeds.

Example: Cygnus X-3 flare

A recent study of a microquasar Cygnus X-3 flare suggests the presence of electron population with a high-energy power-law distribution with energy spectral index $\sigma \approx 1.77$. [11] Let us apply the wave transmission scenario to see what would be required for the physical properties if such a spectrum would be produced by a simple strong step shock moving with the deduced speed $V_1 = 0.63 c$ into a low-density plasma with pre-existing Kolmogorov type turbulence. In the following we set $c = 1$, and follow the transmission analysis presented in detail in [4, 5].

Inverting the equation for $\sigma(r)$ to $r(\sigma)$ we can see that if the $\sigma = 1.77$ is assumed to be due to first-order process, compression ratio of $r_k \approx 4.90$ would be needed.¹ Describing the plasma as a dissipation-free ideal gas, the compression ratio

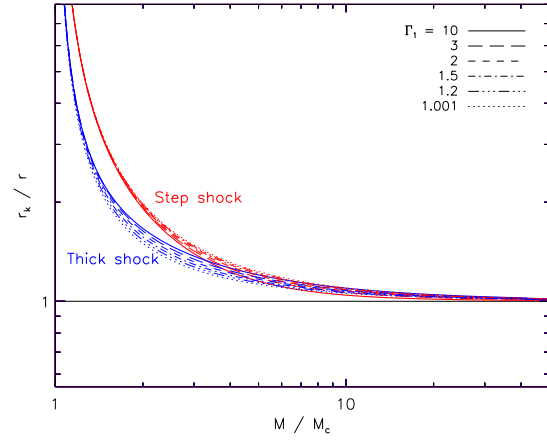


Figure 2: Same as Fig. 1 but for $H_{c1} = -1$ and $q = 2$.

of the flow itself is only $r_{\text{flow}} \approx 3.78$, so the scattering-centre compression ratio would have to be $r_k/r_{\text{flow}} \approx 1.24$ times that of the flow.

From Fig. 1 we can see that this kind of increased compression in the case of a mildly relativistic step shock could follow if the ratio of Alfvénic Mach number to the critical Mach number $M_c = \sqrt{r_{\text{flow}}}$ is $M/M_c \approx 2.74 \Rightarrow M \approx 2.74\sqrt{r_{\text{flow}}} \approx 5.33$. Now, combining the equations for the Alfvénic proper speed and the Mach number, we get the magnetic field: $B = \Gamma_1 V_1 \sqrt{4\pi\mu n}/M$.

For a strong shock the pressure of the upstream gas is negligible to its rest energy, so the specific enthalpy becomes $\mu = m$, where the mass m depends on the composition of the plasma: $m = m_p + m_e$ for hydrogen plasma, and $m = 2m_e$ for electron-positron pair plasma. As neither the composition nor the number density is well known, we use $n = 1 \text{ cm}^{-3}$. Substituting the values in to the equation of the magnetic field, we get $B_H \approx 21 \text{ mG}$ and $B_{\text{pair}} \approx 0.69 \text{ mG}$. Both agree well with the upper limits $B < 0.15 \text{ G}$ deduced from observations of [12], so with the aforementioned assumptions the increased compression ra-

1. Note that the equation for spectral index is not accurate for other than the simplest nonrelativistic shocks – for faster speeds it overestimates the required compression. This value is still illustrative as it sets even stricter limits for the magnetic field. Furthermore, the nonrelativistic formula for diffusive acceleration has been observed to work rather well even in relativistic shocks if increased compression is present. [6]

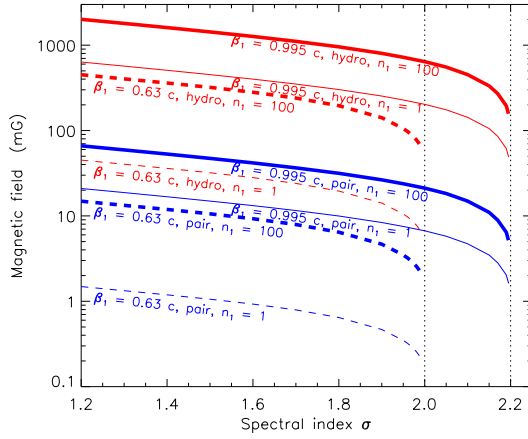


Figure 3: Resulting particle spectral index σ from parallel step shocks when the upstream turbulence ($q = 5/3$, $H_{c1} = 0$) is transmitted through a step shock and the resulting effective compression ratio is used for acceleration. Solid lines are for a relativistic shock moving with speed $V_1 = 0.995 c$, dashed lines correspond to $V_1 = 0.63 c$ (Cyg X-3); upstream number densities are $n = 1 \text{ cm}^{-3}$ and 100 cm^{-3} (thin and thick lines, respectively) The two vertical dotted lines mark the limit for frozen-in turbulence.

tio due to turbulence transmission could play a role in explaining the hard spectrum. It is interesting to note that if the value 100 cm^{-3} [12] is used for the upstream number density, the fields become $B_H \approx 0.21 \text{ G}$ and $B_{\text{pair}} \approx 6.9 \text{ mG}$, rising the B_H beyond the upper limit. More detailed knowledge of the plasma composition and the magnetic field could yield a tool for testing this model for both the improving and rebuttal purposes.

The relation between the spectral index and the magnetic field is shown in Fig. 3 for the Cyg X-3 case and additionally for a fully relativistic shock with $\Gamma_1 \approx 10$, and for densities 1 and 100 cm^{-3} .

Conclusions

I have discussed particle acceleration by the first-order Fermi acceleration mechanism leaving out the simplifying assumption of frozen-in turbulence. I have described the basic results of Alfvén wave transmission analysis [3–8], and the requirements for it to have significant changes in the accelerated particle spectrum, with emphasis on the possibility of having a natural way for parallel shocks to produce spectra steeper than the “uni-

versal” $\sigma \approx 2.2$ value. I have also demonstrated that the physical properties required can be close to those observed, suggesting that this kind of mechanism could indeed be active in certain sources.

I also stress that the mechanisms discussed rely on various assumptions. First of all, the current theory only deals with parallel shocks. It also neglects the particle–wave, wave–shock and wave–wave interactions, and assumes the turbulence to consist of small-amplitude Alfvén waves. Furthermore, the short and long wavelength waves (and particle scattering off them) are treated separately, although it is probable for any real astrophysical shock to affect waves of all lengths. Finally, the second-order Fermi acceleration, very likely to affect the produced spectra, is not considered here, as its connection to the transmission analysis has been studied elsewhere. [13]

References

- [1] P. Schneider, J. G. Kirk, A&A 217 (1989) 344–350.
- [2] J. Virtanen, R. Vainio, Proc. 28th ICRC OG 1.4 (2003) 2023–.
- [3] R. Vainio, R. Schlickeiser, A&A 331 (1998) 793–799.
- [4] R. Vainio, J. J. P. Virtanen, R. Schlickeiser, A&A 409 (2003) 821–829.
- [5] R. Vainio, J. J. P. Virtanen, R. Schlickeiser, A&A 431 (2005) 7.
- [6] J. J. P. Virtanen, R. Vainio, A&A 439 (2005) 461–464.
- [7] J. Tammi, R. Vainio, A&A 460 (2006) 23–28.
- [8] J. Tammi (né Virtanen), Ph.D. thesis, University of Turku (May 2006).
- [9] A. R. Bell, MNRAS 182 (1978) 147–156.
- [10] T. Laitinen, Astrophysics and Space Sciences Transactions 1 (2005) 35–43.
- [11] E. Lindfors, M. Türlér, D. Hannikainen, G. Pooley, J. Tammi, S. Trushkin, E. Valtaoja, A&A, *in press*, astro-ph/0707.2808.
- [12] J. C. A. Miller-Jones, K. M. Blundell, M. P. Rupen, A. J. Mioduszewski, P. Duffy, A. J. Beasley, ApJ 600 (2004) 368–389.
- [13] J. J. P. Virtanen, R. Vainio, ApJ 621 (2005) 313–323.